HHS Public Access

Author manuscript

Small. Author manuscript; available in PMC 2021 April 26.

Published in final edited form as:

Small. 2020 May ; 16(21): e2000963. doi:10.1002/smll.202000963.

Inflammation increases susceptibility of human small airway epithelial cells to pneumonic nanotoxicity

Zhuoran Wu[†],
School of Materials Science and Engineering, Nanyang Technological University, 50 Nanyang Avenue, 639798, Singapore

Pujiang Shi[†],
School of Materials Science and Engineering, Nanyang Technological University, 50 Nanyang Avenue, 639798, Singapore

Hong Kit Lim,
School of Materials Science and Engineering, Nanyang Technological University, 50 Nanyang Avenue, 639798, Singapore

Yiyuan Ma,
School of Materials Science and Engineering, Nanyang Technological University, 50 Nanyang Avenue, 639798, Singapore

Magdiel Inggrid Setyawati,
School of Materials Science and Engineering, Nanyang Technological University, 50 Nanyang Avenue, 639798, Singapore

Dimitrios Bitounis,
Department of Environmental Health, School of Public Health, Harvard University, 665 Huntington Avenue, 02115, Boston, MA

Philip Demokritou,
Department of Environmental Health, School of Public Health, Harvard University, 665 Huntington Avenue, 02115, Boston, MA

Kee Woei Ng,
School of Materials Science and Engineering, Nanyang Technological University, 50 Nanyang Avenue, 639798, Singapore

Department of Environmental Health, School of Public Health, Harvard University, 665 Huntington Avenue, 02115, Boston, MA

Environmental Chemistry and Materials Centre, Nanyang Environment & Water Research Institute, 1 Cleantech Loop, CleanTech One, 637141, Singapore

Skin Research Institute of Singapore, 8A Biomedical Grove, 138648, Singapore

CYTAY@ntu.edu.sg.
[†]Zhuoran Wu and Pujiang Shi should be considered as joint first authors

Supporting information
Experimental methods and supplementary figures are provided in supporting information document available from Wiley Online Library.

Chor Yong Tay
School of Materials Science and Engineering, Nanyang Technological University, 50 Nanyang Avenue, 639798, Singapore

School of Biological Sciences, Nanyang Technological University, 637551, Singapore

Environmental Chemistry and Materials Centre, Nanyang Environment & Water Research Institute, 1 Cleantech Loop, CleanTech One, 637141, Singapore

Abstract

Exposure to inhaled anthropogenic nanomaterials (NM) with dimension < 100nm has been implicated in numerous adverse respiratory outcomes. Although studies have identified key NM physiochemical determinants of pneumonic nanotoxicity, the complex interactive and cumulative effects of NM exposure, especially in individuals with pre-existing inflammatory respiratory diseases remains unclear. Herein, the susceptibility of primary human small airway epithelial cells (SAEC) exposed to a panel of reference NM namely, CuO, ZnO, mild steel welding fume (MSWF) and nano fractions of copier center particles (Nano-CCP), were examined in normal and tissue necrosis factor alpha (TNF-α) induced inflamed SAEC. Compared to normal SAEC, inflamed cells displayed an increased susceptibility to NM-induced cytotoxicity by approximately 15 – 70% due to a higher basal level of intracellular reactive oxygen species (ROS). Among the NM screened, ZnO, CuO and Nano-CCP were observed to trigger an over-compensatory response in normal SAEC, resulting in an increased tolerance against subsequent oxidative insults. However, the inflamed SAEC failed to adapt to the NM exposure due to an impaired nuclear factor erythroid 2-related factor 2 (Nrf2) mediated cytoprotective response. Our findings revealed that susceptibility to pulmonary nanotoxicity is highly dependent on the interplay between NM properties and inflammation of the alveolar milieu.

Graphical Abstract

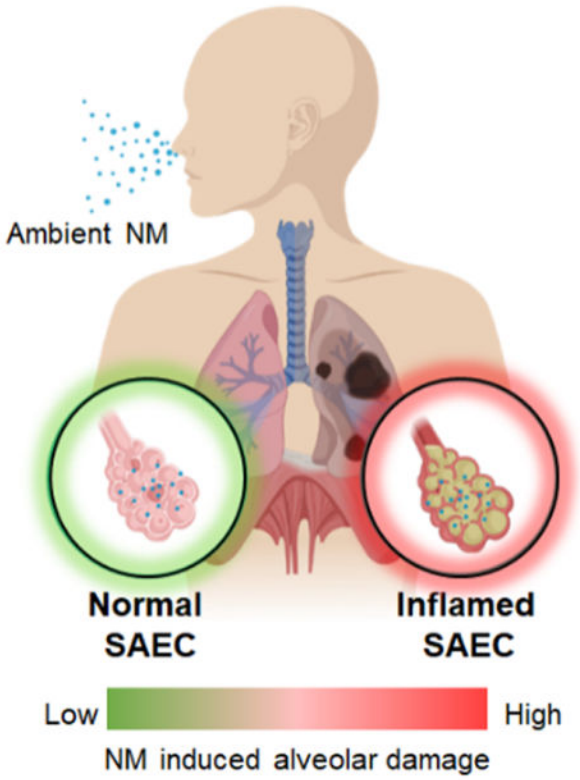

Primary human small airway epithelial cells (SAEC) in its inflamed state is more susceptible to the cytotoxic effects of ambient anthropogenic nanomaterials (NM) exposure (i.e. CuO, ZnO, mild steel welding fume (MSWF) and nano fractions of copier center particles (Nano-CCP)). An inflamed milieu induces a higher basal level of intracellular ROS level and desensitizes the Nrf-2-mediated cytoprotective signaling pathways.

Keywords

Nanotoxicology; lung inflammation; reactive oxygen species; cellular adaptation; Nrf2 stress response

Anthropogenic nanomaterials (NM) can be broadly defined as materials with at least one dimension that is < 100 nm, which are either produced as a result of human influence (i.e. incidental nanomaterials) or purposefully designed and manufactured by human (i.e. engineered NM).[1] Examples of engineered NM include metal-based NM such as TiO_2, ZnO, Ag, CuO, that are commonly incorporated in a wide range of consumer goods[2–3], whereas incidental NM may be generated from activities such as steel welding, printing and vaping (e-cigarette).[4–6] Due to their increased demand and rampant production, the annual flux of anthropogenic NM circulating within our earth system was estimated to be in the astonishing range of 1–10 million metric tons/ year.[1] Because of their ubiquitous presence in the environment, human exposure to NM by means of inhalation in our everyday life is inadvertent.[7] Consequently, this has raised significant public health concerns since these extremely small entities are readily respired and have been documented to bypass different

types of biological barriers and interact extensively with biomolecules, cells and even tissues, leading to various adverse toxic outcomes.[8–11]

In the past two decades, the majority of the pulmonary nanotoxicological studies were mostly based on the structure-activity relationship (SAR)-based risk assessment framework as the standard *modus operandi* to elucidate the possible adverse effects of NM exposure.[12] Specifically, there is a strong emphasis on the identification of key physiochemical materials properties[13] such as particle size[14], shape[8], chemistries[15], surface charge[16], porosity[17] in determining the toxic potential of NM. From these studies, many critical mechanistic insights and safer-by-design rules have been obtained.[18] However, even when normalized to the same particle type with identical materials-centric characteristics, the adverse effects of NM may not be equally distributed among population groups and individuals, especially in persons with pre-existing inflammatory diseases. Differences in susceptibility and vulnerability to NM exposure may have a large disproportionate effect on the health of certain populations.[19] Therefore, there is considerable value in understanding how NM exposure may differentially affect population subgroups, an area that is important yet critically overlooked in contemporary nanotoxicology.

As a counterpoint to the nearly exclusive focus on the SAR approach, we focus on examining both the acute (high dose) and sub-chronic (low dose) nanotoxicological response as a function of the state of inflammation in SAEC. Lungs of individuals with asthma, chronic obstructive pulmonary disease (COPD) and pulmonary fibrosis are characterized by a persistent state of inflammation.[20] To establish an *in vitro* model mimicking chronically inflamed SAEC, the cells were subjected to a week-long treatment of TNF-α (10 ng/ml), a potent inflammatory cytokine that is overexpressed within the alveolar milieu of numerous pulmonary inflammatory diseases.[21] Compared to the healthy control, the TNF-α treated cells displayed significant upregulation of mRNA transcripts such as GM-CSF, TNF-α, IL-6, IL-8, (Figure S1A) as well as robust expression of α-SMA, fibronectin, and vimentin (Figure S1B), all of which are hallmark inflammatory and pathological markers observed in patients with functional respiratory impairment.[22–23]

Model reference NM including ZnO, CuO, mild steel welding fume (MSWF), and nano-copier centre particles (Nano-CCP) were chosen as representative ambient NM, which have previously been identified as possible nano-agents of occupational lung injuries.[24–26] The physiochemical properties of the panel NM[27–29] were characterized using transmission electron microscope (TEM), dynamic light scattering (DLS) and zeta potential measurement. Broadly speaking, the NM are mostly spherical with a certain degree of irregularity (Figure S2). The primary particle size of the NM is generally less than or close to 100 nm (Table S1). Conversely, the hydrodynamic particle (D_H) sizes of the respective NM measured in water and complete cell culture medium were significantly larger. This could be attributed to the presence of hydration layer and non-specific binding of micro-nutrients, salt content and serum proteins, which could lead to inter-molecular bridging of the NM.[30] Zeta potential measurements revealed that ZnO and MSWF possess a positive surface charge (6.3 and 25.7 mV respectively) whereas Nano-CCP and CuO were negatively charged (−33.7 and −21.3 mV respectively) in water. However, when the NM were dispersed in the complete growth medium, the surface of the NM now bears a net negative charge of

varying magnitudes that ranges from ~ 9–25 mV. The charge reversal observed in ZnO and MSWF is indicative of the formation of protein corona on the NM surface.[31]

We next compared the acute cytotoxic response of normal SAEC and inflamed SAEC against the panel of NM. In general, in both cell types, we observed a decline in cell viability in a dose-dependent manner (Figure1A–D). In the case of normal SAEC, the approximated LD_{50} of the respective NM are-ZnO: 18 μg/ml; CuO: 50 μg/ml; and MSWF: 400 μg/ml, whereas the LD_{50} for Nano-CCP was beyond the experimental dose range, as the viability was only reduced by ~ 40% at the highest concentration of Nano-CCP used (i.e. 100 μg/ml). Similar toxicity results of Nano-CCP were also observed in a previous study involving SAEC.[29] Accordingly, the toxicity of the panel NM can then be ranked as follows: ZnO > CuO > Nano-CCP > MSWF. Differences in the toxic potential of the respective NM could in part be explained by their relative ease of dissolution inside the cells. Numerous studies have shown that ZnO and CuO NM are highly soluble in the acidic lysosomal compartment, which could lead to the release of excess intracellular Zn^{2+} and Cu^{2+} ions to induce a potent cytotoxic effect.[32–33] Comparatively, Nano-CCP and MSWF are less soluble,[34–35] but they are inherently more complex in terms of composition.[36] In contrast to the normal counterpart, inflamed SAEC were clearly more susceptible to NM exposure, as evidenced by an approximately 15–70% decrease in LD_{50} across the tested NM. To the best of our knowledge, our findings represent the first experimental proof that implicates cellular inflammatory state as a critical bio-determinant that will skew the NM induced cytotoxic effects in SAEC.

Acute and chronic inflammatory respiratory diseases have been correlated with oxidative damage and increased levels of H_2O_2 in exhaled breath condensate of patients.[37] NM are known to incur nanotoxicity to cells by generating oxidative stress.[10, 38–39] Therefore, we postulated that the weakening of the inflamed cells to the NM treatment may be due to its dysregulated state of redox homeostasis, thereby leading to a heightened sensitivity to NM oxidative insults. To discern the basal redox status, cells were counter-stained with CellROX Green, which will enable us to detect and quantify the intracellular reactive oxygen species (ROS) level. In support of our postulation, we observed pronounced difference in the ROS expression in both cell types (Figure 1E), with the inflamed cells exhibiting a 5-fold higher expression of intracellular ROS (Figure 1F).

When we measured the Trolox equivalent total antioxidant capacity (TAC) of both cell types, the antioxidant capacity of inflamed cells was significantly lower, by approximately 50% compared to the healthy control (Figure 1G). Our findings are consistent with earlier reports relating to the depletion of antioxidants in lung epithelium and alveolar macrophages of COPD patient.[39] In addition to the antioxidant mechanism, the ubiquitin proteasome system (UPS), a major lysosomal protein-degradation machinery, has been also identified as an important molecular player in the pathobiology of lung inflammation and injuries.[40–41] Dysfunction of the UPS can lead to the accumulation of oxidatively damaged proteins and negatively impact cell viability.[42] Therefore, we next compared the chymotrypsin-like activity of the proteasome by measuring the degradation of the fluorogenic peptide, Suc-LLVY-AMC, in both normal and inflamed SAEC. As shown in Figure 1H, the proteolytic capacity of the inflamed cells is significantly suppressed compared to the healthy cells,

suggesting that the week-long TNF-α treatment can severely disrupt the protein degradation pathways in SAEC. Collectively, the increased ROS level, the reduced levels of antioxidant activity, and the suppressed proteolytic capacity to remove damaged proteins, strongly suggest that the inflamed cells are in a state of oxidative stress, thereby sensitizing the cells to the pro-oxidant effects of NM.

As the first line of defense against inhaled oxidative stress-inducing pollutants and pathogens, the airway epithelium has evolved elaborate adaptive cellular mechanisms to limit oxidative damage.[43–44] For instance, exposing alveolar epithelial cells to nontoxic doses of cigarette smoke extract (CSE) induced oxidative stress-mediated hyper fusion of mitochondria and increased metabolic activity as part of an adaptive pro-survival response.[44] Although we have shown that inflamed cells are pre-disposed to the acute cytotoxic effects of NM, it is unclear how normal and inflamed cells would differentially adapt to non-cytotoxic doses of NM. In order to extend our *in vitro* models for cellular adaptation studies, we next integrated our recently developed 2-step conditioning and challenging (2Cs) protocol into the experimental workflow.[45] Briefly, in step 1, the cells were conditioned with a non-cytotoxic dose of NM for 24h. The number of rounds of conditioning is denoted by the subscript (i.e. C_x). In step 2, cells were challenged with the LD_{50} of tert-Butyl hydroperoxide (TBHP), a well-established oxidant, and cell viability was subsequently measured (Figure 2A). LD_{50} values of TBHP for the normal and inflamed cells were determined respectively in separate experiments (Figure S3). To quantify the adaptive response, we introduced the term adaptive index, which is defined as the normalized viability of the conditioned cells against the unconditioned cells - 1. An adaptive index > 0.2 indicates a positive adaption, since history of NM exposure can lead to increased tolerance against oxidative damage. We termed this NM-induced adaptive response as *nano-adaptation*. Conversely, an adaptive index < −0.2 denotes a NM-induced maladaptive (*nano-maladaptation*) process, as the NM pre-treatment sensitizes the cells to oxidative damage. An adaptive index range of ~ 0.2 to −0.2 (i.e. within 20% change of basal viability data) suggest that the cells are unable to mount an adaptive response to the NM treatment.

As the NM concentration for the cellular adaptation studies is low, coupled with the considerable different D_H the NM displayed in the cell culture medium, it is therefore critical to normalize the observation against the actual delivered dose of the respective NM. For this study, we have chosen to administer a conditioning dose equivalent to 1 μg/ml of ZnO NM, which was previously shown to be capable of triggering an adaptive response.[46] To determine the conditioning doses required for the other NM, we have employed the Harvard-based *in vitro* dosimetry method.[46,47] This method integrates the Harvard Volumetric Centrifugation Method (VCM) to determine the effective density (ρ_{eff}) of the NM agglomerate in the culture medium and the distorted grid (DG) model[46] to allow accurate *in silico* modeling of the time-dependent deposition of NM onto the cell surface. As can be seen from the fractional deposition profile (Figure 2B), only 59% of the ZnO NM was delivered after 24h of NM exposure, and this would correspond to a non-cytotoxic delivered dose of ~ 0.1375 μg/ cm^2 by the end of the conditioning phase. Using the *in vitro* dosimetry data, the administered dose for CuO, MSWF and Nano-CCP were then corrected accordingly so that the delivered dose is constant across the samples.

Interestingly, the adaptive response of the normal SAEC revealed a NM-dependent effect. (Figure 2C) Cells exposed to ZnO, CuO and Nano-CCP were observed to positively adapt to the NM as the cells exhibited a 20–60% increase in adaptive index compared to the unconditioned control. In stark contrast, we did not observe any adaptive response as a result of delivered-dose normalized MSWF treatment. This suggest that exposure to ZnO, CuO and Nano-CCP can trigger an intracellular defense mechanism to trigger an over-compensatory response to NM-induced oxidative stress, which is manifested in the increase in cellular resilience to subsequent oxidative insults. Furthermore, the adaptive response increases with the number of rounds of conditioning in accordance to our earlier study (Figure 2C).[45] We next repeated our adaptation experiment on the inflamed cells and ask weather if the state of inflammation could potentially interfere with the nano-adaptation process. While we did not observe any maladaptation, we noted that the ZnO, CuO and Nano-CCP induced adaptive response was effectively muted in the inflamed cells (Figure 2D). Consistent with the results obtained with the healthy SAECs, adaptative response was also absent for the MSWF conditioned inflamed cells. This implies that a chronically inflamed alveolar milieu can severely interfere and disrupt cellular homeostasis. Our findings strongly suggest that alveolar epithelial cells are intrinsically capable of maximizing its fitness to non-cytotoxic dose of NM exposure via the process of cellular adaption. Such NM-induced adaptive response (nano-adaptation) is highly dependent on both the physiochemical properties of the NM as well as the inflammatory status of the SAEC. From the materials standpoint, it is interesting to note that NM capable of triggering an adaptive response in normal SAEC corresponds to NM with higher toxic (oxidative) potential (Figure 2C).

To gain further mechanistic insights into the NM-induced adaptive response, we next switched our focus to the nuclear factor erythroid 2-like 2 (Nrf2) transcription factor. Nrf2 is a master regulator of antioxidative and cytoprotective responses.[48] Among the > 600 genes[49] that are regulated by the Nrf2 signaling pathway, > 200 encode cytoprotective proteins.[50] Under basal conditions, Nrf2 binds to Kelch-like ECH-associated protein 1 (Keap1), which sequesters Nrf2 in the cytoplasm and facilitate its degradation via the ubiquitin proteasome system (UPS).[51] This phenomenon is aptly reflected in untreated normal SAEC, where the expression of Nrf2 was observed to be limited predominately within the cell cytoplasm (Figure 3A). Upon activation by electrophiles/ oxidative stress, Nrf2 will detach from Keap1 and translocate rapidly into the cell nucleus, where it heterodimerizes with the musculoaponeurotic fibrosarcoma (Maf) proteins and facilitates its binding to the antioxidant responsive element (ARE). This will then promote the upregulation of several phase II xenobiotic metabolizing enzymes, antioxidants, and molecular chaperons to enhance the adaptive cell defense response.[51] Consistent with this paradigm, we observed that the cells exposed to conditioning dose of ZnO, CuO and Nano-CCP displayed intense Nrf2 immunofluorescence signals in the cell nucleus compartment (Figure 3A). In contrast, under the same NM exposure conditions, nuclear translocation of Nrf2 in the inflamed SAEC did not occur. Expression level of nuclear bound Nrf2 was found to be ~ 2-fold higher in the NM-conditioned healthy cells compared to the NM-conditioned inflamed cells (Figure 3B). The lack of Nrf2 nuclear translocation in the inflamed SAEC could potentially point to a desensitized endogenous Nrf2 stress response. Indeed, time-course monitoring of the

intracellular ROS level immediately following CuO, ZnO and Nano-CCP conditioning in normal SAEC, revealed a transient but significant spike (4-fold higher) in ROS level approximately 1 h into the experiment (Figure 3C). This is followed by a gradual decrease in intracellular ROS level which eventually plateaus off from 10 h onwards. In contrast, the basal level of ROS in the NM-conditioned inflamed cells was not elevated compared to the untreated control (Figure 3D). The normalized ROS level can be explained by the increase in TAC in the normal SAEC by approximately 20% after a single round of NM-conditioning, suggesting that the cells were able to sense the NM-induced redox imbalance and increased the production of antioxidants to scavenge the excess ROS (Figure 3E). On the other hand, the TAC of the inflamed cells remained unchanged. Furthermore, we observed a considerable increase in proteolytic capacity of the normal cells exposed to conditioning dose of ZnO, CuO and Nano-CCP by 84%, 30% and 27% respectively compared to the untreated control. Yet again, we noted that the NM-induced proteolytic activation was muted in the inflamed SAEC (Figure 3F). Taken together, our findings showed that the inability of the inflamed cells to adapt to the NM exposure could be attributed in part to the impaired Nrf2 signaling and its mediated cytoprotective responses.

In conclusion, the respiratory nanotoxicological responses of normal and sub-chronically inflamed SAEC to a panel of well-characterized NM (i.e. ZnO, CuO, MSWF and Nano-CCP) was examined. The higher basal oxidative burden of the inflamed SAEC not only increased the susceptibility of the cells to acute toxicity of NM, but also severely dampen the cells ability to adapt to low (non-toxic) doses of NM exposure that is also dependent on the chemical composition of NM. Difference in responsiveness of the Nrf2 stress response pathway was revealed as a key physiological determinant, exacerbating the nanotoxicological responses in inflamed SAEC. Additional research is warranted to examine in greater detail the susceptibility of individuals with pre-existing inflammatory respiratory conditions to ambient NM exposure.

Supplementary Material

Refer to Web version on PubMed Central for supplementary material.

Acknowledgements

The authors gratefully acknowledge support by the Nanyang Technological University - Harvard School of Public Health Initiative for Sustainable Nanotechnology (NTU-Harvard SusNano; NTU-Harvard Initiative for Sustainable Nanotechnology seed grant (Ref. No. NTU-HSPH 18002). Engineered nanomaterial used in the research presented in this publication have been synthesized, characterized, and provided by the Engineered Nanomaterials Resource and Coordination Core established at Harvard T. H. Chan School of Public Health (NIH grant # U24ES026946) as part of the Nanotechnology Health Implications Research (NHIR) Consortium.

References

1. Hochella MF Jr.; Mogk DW; Ranville J; Allen IC; Luther GW; Marr LC; McGrail BP; Murayama M; Qafoku NP; Rosso KM; Sahai N; Schroeder PA; Vikesland P; Westerhoff P; Yang Y, Science 2019, 363 (6434).
2. Tan MH; Commens CA; Burnett L; Snitch PJ, Australas J Dermatol 1996, 37 (4), 185–7. [PubMed: 8961584]
3. Yokel RA; Macphail RC, J Occup Med Toxicol 2011, 6, 7. [PubMed: 21418643]

4. Cena LG; Keane MJ; Chisholm WP; Stone S; Harper M; Chen BT, J Occup Environ Hyg 2014, 11 (12), 771–80. [PubMed: 24824154]
5. Scungio M; Vitanza T; Stabile L; Buonanno G; Morawska L, Sci Total Environ 2017, 586, 623–630. [PubMed: 28196755]
6. Son Y; Mainelis G; Delnevo C; Wackowski OA; Schwander S; Meng Q, Chem Res Toxicol 2019, 32(6), 1087–1095 [PubMed: 30977360]
7. Poh TY; Ali N; Mac Aogain M; Kathawala MH; Setyawati MI; Ng KW; Chotirmall SH, Part Fibre Toxicol 2018, 15 (1), 46. [PubMed: 30458822]
8. Oh WK; Kim S; Yoon H; Jang J, Small 2010, 6 (7), 872–9. [PubMed: 20209653]
9. Wang Y; Chen Z; Ba T; Pu J; Chen T; Song Y; Gu Y; Qian Q; Xu Y; Xiang K; Wang H; Jia G, Small 2013, 9 (9–10), 1742–52. [PubMed: 22945798]
10. Setyawati MI; Tay CY; Leong DT, Biomaterials 2013, 34 (38), 10133–42. [PubMed: 24090840]
11. Giovanni M; Tay CY; Setyawati MI; Xie J; Ong CN; Fan R; Yue J; Zhang L; Leong DT, Environ Toxicol 2015, 30 (12), 1459–69. [PubMed: 24930694]
12. Cai X; Dong J; Liu J; Zheng H; Kaweeteerawat C; Wang F; Ji Z; Li R, Nat Commun 2018, 9 (1), 4416. [PubMed: 30356046]
13. Tay CY; Setyawati MI; Xie J; Parak WJ; Leong DT, Advanced Functional Materials 2014, 24 (38), 5936–5955.
14. Chen LQ; Fang L; Ling J; Ding CZ; Kang B; Huang CZ, Chem Res Toxicol 2015, 28 (3), 501–9. [PubMed: 25602487]
15. Das B; Tripathy S; Adhikary J; Chattopadhyay S; Mandal D; Dash SK; Das S; Dey A; Dey SK; Das D; Roy S, J Biol Inorg Chem 2017, 22 (6), 893–918. [PubMed: 28643149]
16. Frohlich E, Int J Nanomedicine 2012, 7, 5577–91. [PubMed: 23144561]
17. Tay CY; Setyawati MI; Leong DT, ACS Nano 2017, 11 (3), 2764–2772. [PubMed: 28287706]
18. Yan L; Zhao F; Wang J; Zu Y; Gu Z; Zhao Y, Adv Mater 2019, 31 (45), e1805391. [PubMed: 30701603]
19. Chen Z; Meng H; Xing G; Yuan H; Zhao F; Liu R; Chang X; Gao X; Wang T; Jia G; Ye C; Chai Z; Zhao Y, Environ Sci Technol 2008, 42 (23), 8985–92. [PubMed: 19192829]
20. Ichinose M, Allergol Int 2009, 58 (3), 307–13. DOI 10.2332/allergolint.09-RAI-0106. [PubMed: 19628975]
21. Yao Y; Zhou J; Diao X; Wang S, Ther Adv Respir Dis 2019, 13, 1753466619866096.
22. Yende S; Waterer GW; Tolley EA; Newman AB; Bauer DC; Taaffe DR; Jensen R; Crapo R; Rubin S; Nevitt M; Simonsick EM; Satterfield S; Harris T; Kritchevsky SB, Thorax 2006, 61 (1), 10–6. [PubMed: 16284220]
23. Tsantikos E; Lau M; Castelino CM; Maxwell MJ; Passey SL; Hansen MJ; McGregor NE; Sims NA; Steinfort DP; Irving LB; Anderson GP; Hibbs ML, J Clin Invest 2018, 128 (6), 2406–2418. [PubMed: 29708507]
24. Pirela S; Molina R; Watson C; Cohen JM; Bello D; Demokritou P; Brain J, Inhal Toxicol 2013, 25 (9), 498–508. [PubMed: 23895351]
25. Rossner P; Vrbova K; Strapacova S; Rossnerova A; Ambroz A; Brzicova T; Libalova H; Javorkova E; Kulich P; Vecera Z; Mikuska P; Coufalik P; Krumal K; Capka L; Docekal B; Moravec P; Sery O; Misek I; Fictum P; Fiser K; Machala M; Topinka J, Toxicol Sci 2019, 168 (1), 190–200. [PubMed: 30500950]
26. Ahamed M; Akhtar MJ; Alhadlaq HA; Alrokayan SA, Nanomedicine (Lond) 2015, 10 (15), 2365–77. [PubMed: 26251192]
27. Setyawati MI; Singh D; Krishnan SPR; Huang X; Wang M; Jia S; Goh BHR; Ho CG; Yusoff R; Kathawala MH; Poh TY; Ali N; Chotirmall SH; Aitken RJ; Riediker M; Christiani DC; Fang M; Bello D; Demokritou P; Ng KW, Environ Sci Technol 2020.
28. Eweje F; Ardoña HAM; Zimmerman JF; O'Connor BB; Ahn S; Grevesse T; Rivera KN; Bitounis D; Demokritou P; Parker KK, Nanoscale 2019, 11 (38), 17878–17893. [PubMed: 31553035]
29. Pirela SV; Miousse IR; Lu X; Castranova V; Thomas T; Qian Y; Bello D; Kobzik L; Koturbash I; Demokritou P, Environ Health Perspect 2016, 124 (2), 210–9. [PubMed: 26080392]

30. Moore TL; Rodriguez-Lorenzo L; Hirsch V; Balog S; Urban D; Jud C; Rothen-Rutishauser B; Lattuada M; Petri-Fink A, Chem Soc Rev 2015, 44 (17), 6287–305. [PubMed: 26056687]
31. Wu F; Harper BJ; Harper SL, Environ Toxicol Chem 2019, 38 (3), 591–602. [PubMed: 30615210]
32. Henson TE; Navratilova J; Tennant AH; Bradham KD; Rogers KR; Hughes MF, Nanotoxicology 2019, 13 (6), 795–811. [PubMed: 30938207]
33. Antonini JM; Lawryk NJ; Murthy GG; Brain JD, J Toxicol Environ Health A 1999, 58 (6), 343–63. [PubMed: 10580758]
34. Pirela SV; Martin J; Bello D; Demokritou P, Crit Rev Toxicol 2017, 47 (8), 678–704. [PubMed: 28524743]
35. Han KN; Fuerstenau MC, International Journal of Mineral Processing 2003, 72 (1–4), 355–364.
36. Dekhuijzen PN; Aben KK; Dekker I; Aarts LP; Wielders PL; van Herwaarden CL; Bast A, Am J Respir Crit Care Med 1996, 154 (3 Pt 1), 813–6. [PubMed: 8810624]
37. Setyawati MI; Tay CY; Bay BH; Leong DT, ACS Nano 2017, 11 (5), 5020–5030. [PubMed: 28422481]
38. Nguyen KT; Wu Z; Huang T; Tay CY, Curr Med Chem 2018, 25 (12), 1420–1432. [PubMed: 28403790]
39. MacNee W, Proc Am Thorac Soc 2005, 2 (1), 50–60. [PubMed: 16113469]
40. Shim SM; Lee WJ; Kim Y; Chang JW; Song S; Jung YK, Cell Rep 2012, 2 (3), 603–15. [PubMed: 22921402]
41. Lim KL, Expert Rev Proteomics 2007, 4 (6), 769–81. [PubMed: 18067415]
42. Yoshida K; Gowers KHC; Lee-Six H; Chandrasekharan DP; Coorens T; Maughan EF; Beal K; Menzies A; Millar FR; Anderson E; Clarke SE; Pennycuick A; Thakrar RM; Butler CR; Kakiuchi N; Hirano T; Hynds RE; Stratton MR; Martincorena I; Janes SM; Campbell PJ, Nature 2020.
43. Cantin AM, Proc Am Thorac Soc 2010, 7 (6), 368–75. [PubMed: 21030515]
44. Ballweg K; Mutze K; Konigshoff M; Eickelberg O; Meiners S, Am J Physiol Lung Cell Mol Physiol 2014, 307 (11), L895–907. [PubMed: 25326581]
45. Wu Z; Yang H; Archana G; Rakshit M; Ng KW; Tay CY, Nanotoxicology 2018, 12 (10), 1215–1229. [PubMed: 30428752]
46. DeLoid GM; Cohen JM; Pyrgiotakis G; Demokritou P, Nat Protoc 2017, 12 (2), 355–371. [PubMed: 28102836]
47. Nguyen T; Nioi P; Pickett CB, J Biol Chem 2009, 284 (20), 13291–5. [PubMed: 19182219]
48. Malhotra D; Portales-Casamar E; Singh A; Srivastava S; Arenillas D; Happel C; Shyr C; Wakabayashi N; Kensler TW; Wasserman WW; Biswal S, Nucleic Acids Res 2010, 38 (17), 5718–34. [PubMed: 20460467]
49. Hayes JD; Dinkova-Kostova AT, Trends Biochem Sci 2014, 39 (4), 199–218. [PubMed: 24647116]
50. Villeneuve NF; Lau A; Zhang DD, Antioxid Redox Signal 2010, 13 (11), 1699–712. [PubMed: 20486766]
51. Li W; Yu S; Liu T; Kim JH; Blank V; Li H; Kong AN, Biochim Biophys Acta 2008, 1783 (10), 1847–56. [PubMed: 18585411]

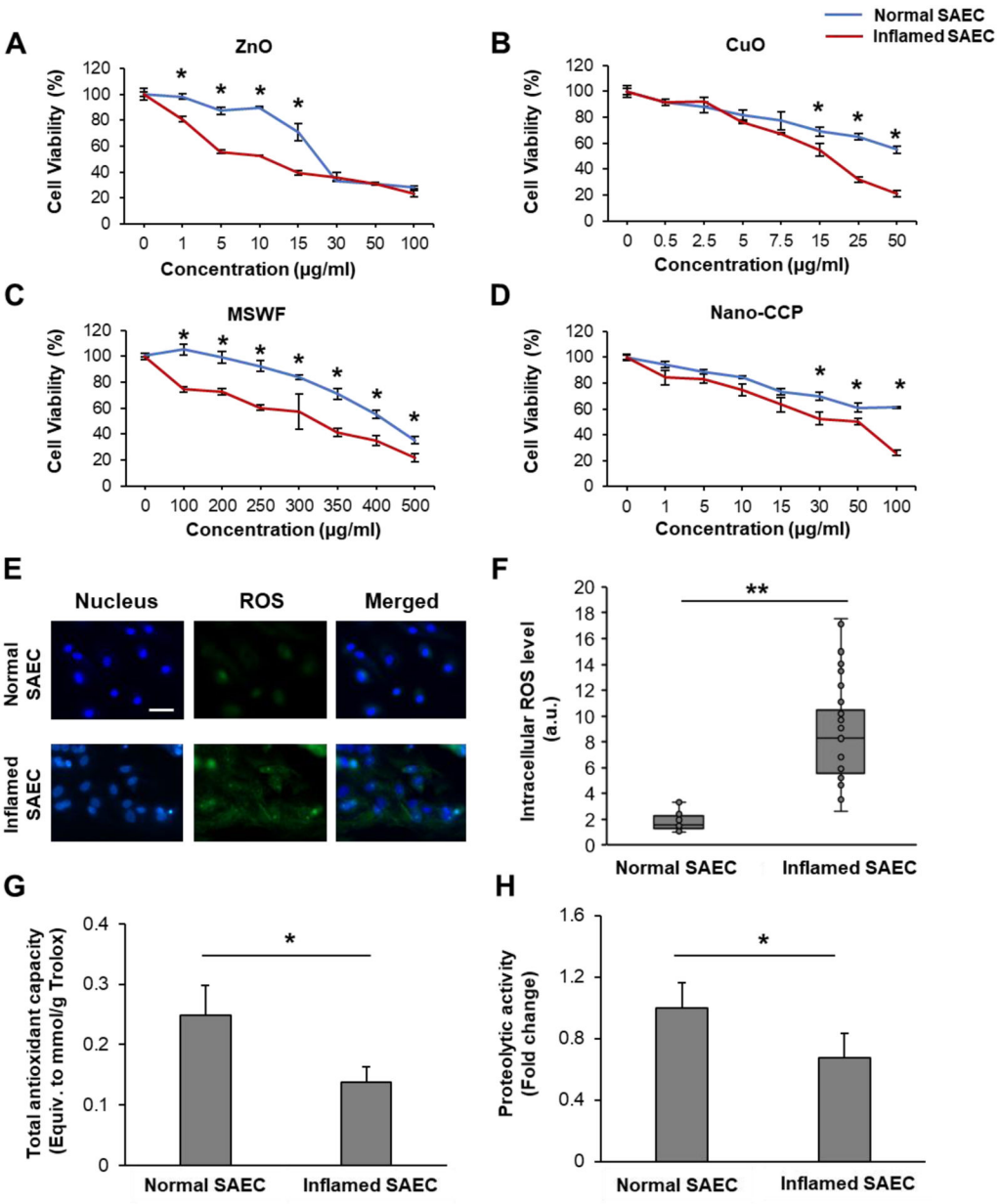

Figure 1. Inflamed SAEC are more susceptible to NM-induced cytotoxicity.

Dose-response graphs for normal and inflamed SAEC exposed to (A) ZnO, (B) CuO, (C) MSWF and (D) Nano-CCP. (E) Representative fluorescence images of normal and inflamed SAEC counterstained for intracellular ROS (green) using CELLROX Green. Cell nucleus (blue) was labeled using Hoechst 33342 dye. Scale bar = 50 μm. (F) Mean intracellular ROS level of both normal and inflamed SAEC. n= 20 per group. Mean (G) total antioxidant capacity and (H) proteolytic activity in normal and inflamed SAEC. Experiments were conducted in triplicates. Data are presented as mean ± SD. * and ** denote statistical significance between experimental groups. *: $p < 0.05$, and **: $p < 0.01$.

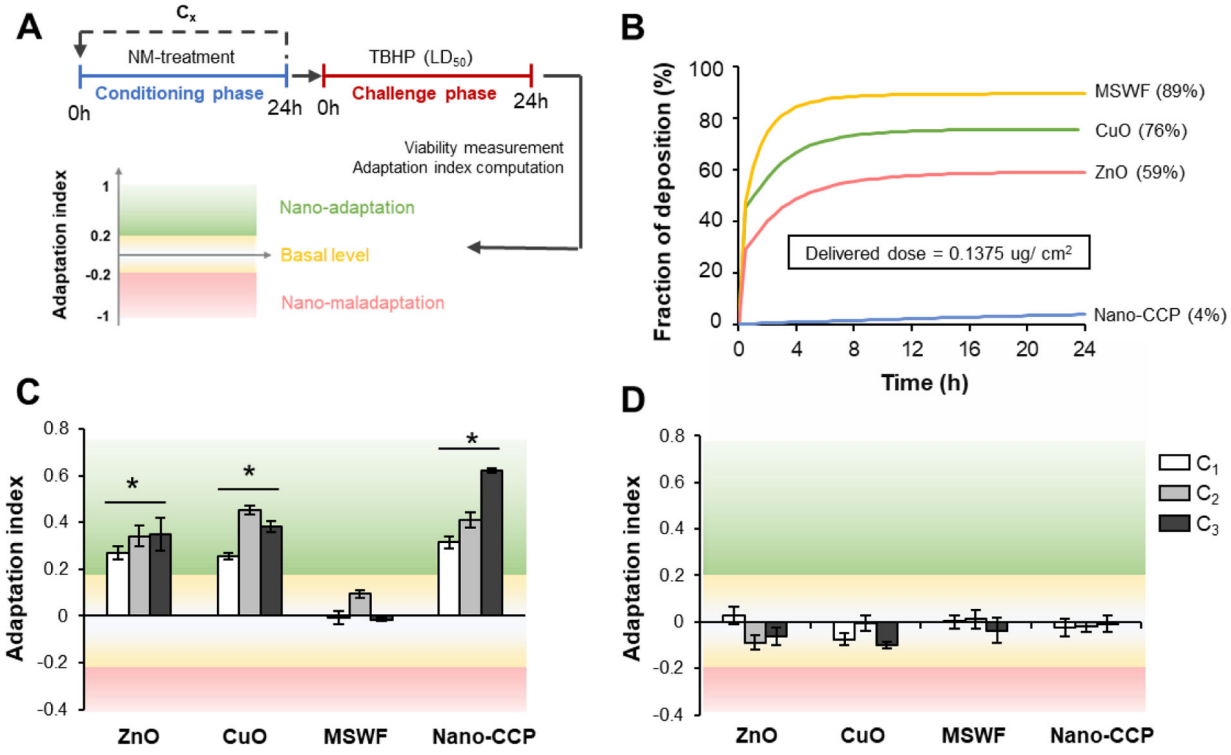

Figure 2. Nano-adaptation is dependent on NM composition and inflammatory status of SAEC.

(A) Schematic to illustrate the conditioning and challenge (2Cs) experimental workflow and definition of the various possible nano-adaptive outcomes. (B) Determination of fraction of deposited NM over 24 h using the Harvard *in vitro* dosimetry method. An equivalent delivered dose of 0.135 μg/cm^2 was used for all the tested NM in this study. The corrected administered dose used for ZnO, CuO, MSWF, and Nano-CCP are 1, 0.8, 0.7, 14.6 μg/ml, respectively. Computed adaptation indices of (C) normal and (D) inflamed SAEC after multiple rounds of conditioning. Experiments were conducted in triplicates. Data are presented as mean ± SD. * denotes statistical significance between the NM conditioned and the untreated control group. *: $p < 0.05$.

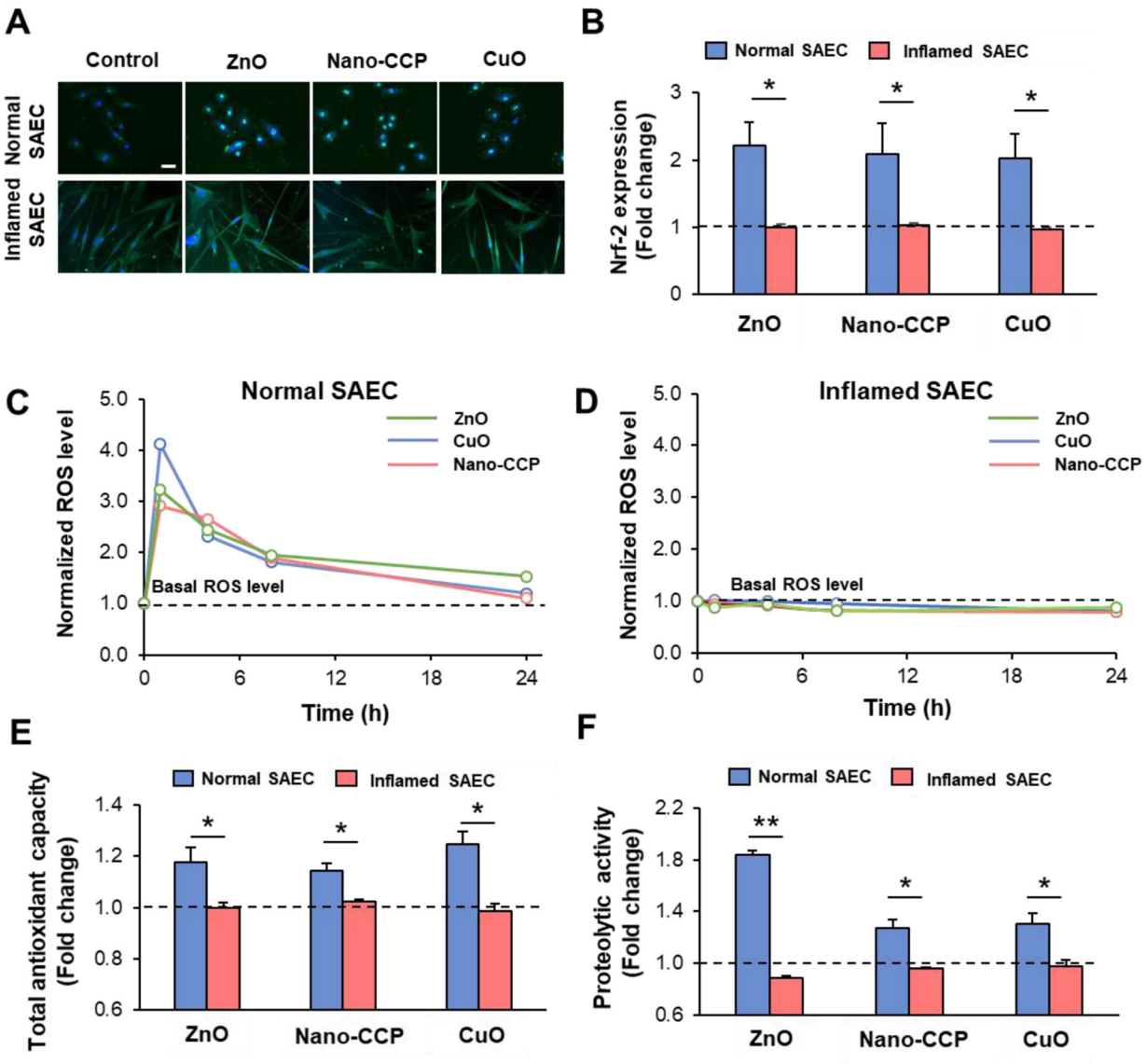

Figure 3. Defective Nrf2-dependent ROS signaling in inflamed SAEC deregulates nano-adaptive response.

(A) Representative immunofluorescence images of ZnO, CuO, and Nano-CCP conditioned (24h) normal and inflamed SAEC counterstained for Nrf2 (green). Cell nucleus (blue) was labeled using Hoechst 33342 dye. Scale bar = 50 μm. (B) Normalized expression of cell nucleus-bound Nrf-2 in normal and inflamed SAEC. n=20 per group. Time-course measurement of intracellular ROS level in (C) normal and (D) inflamed SAEC exposed to ZnO, CuO and Nano-CCP over 24h of NM treatment time. Mean (E) total antioxidant capacity and (F) proteolytic activity in normal and inflamed SAEC 24h post NM conditioning. Experiments were conducted in triplicates. Data are presented as mean ± SD. * and ** denote statistical significance between experimental groups. *: $p < 0.05$, and **: $p < 0.01$.